Regulation of *flotillin-1* in the establishment of NIH-3T3 cell–cell interactions[1]

Pedro P. López-Casas, Jesús del Mazo*

Department of Cell and Developmental Biology, Centro de Investigaciones Biológicas, Ramiro de Maeztu 9, 28040 Madrid, Spain

Received 8 September 2003; revised 15 October 2003; accepted 15 October 2003

First published online 4 November 2003

Edited by Beat Imhof

Abstract **Flotillin-1 is a lipid raft-associated protein involved in neuronal regeneration, insulin signaling in adipocytes, and phagosome maturation in macrophages. We detected abundant *flotillin-1* mRNA expression in confluent cultures of mouse NIH-3T3 fibroblasts. These cells were used as a model to assess the regulation of *flotillin-1* mRNA and protein expression by cell–cell interactions. The disruption of cell–cell interactions triggered the downregulation of the *flotillin-1* gene. However, the establishment of new cell interactions, and finally confluence, increased both the flotillin-1 transcript and its protein. Despite flotillin-1 having been described as an integral protein of the cell membrane, it is also very conspicuous in the hydrophilic fraction (the non-membrane fraction) of confluent cell extracts. The promoter region of the *flotillin-1* gene was isolated and analyzed by transfection experiments, and the regulatory domains containing motifs for binding transcription factors involved in cell differentiation were identified.**

Key words: *flotillin-1*; *reggie-2*; Lipid raft; Cell–cell interaction; *flo-1* promoter

1. Introduction

Lipid rafts are dynamic subdomains of the plasma membrane enriched in specific, highly ordered glycosphingolipids and cholesterol – molecules that confer the biophysical properties that allow their purification [1]. Lipid rafts can recruit a multitude of proteins including glycosylphosphatidylinositol-anchored proteins and acylated proteins such as the Src family kinases and the caveolins. Caveolins are components of special, flask-shaped lipid rafts – the caveolae [2].

Lipid rafts are involved in important cell processes such as the polarized sorting of apical membrane proteins in epithelial cells and signal transduction [3]. They also participate in the assembly of cell adhesion complexes in which the actin cytoskeleton is involved [4]. Cell adhesion complexes are critical for the physical coordination of cell interactions.

The proteins of the flotillin/reggie family are important components of lipid rafts. Although both flotillins and caveolins were recently described as novel constituents of raft domains and caveolae [5,6], flotillins are present in cells that lack morphologically definable caveolae and have been localized in non-caveolar membranes [7,8]. Reggie-1 and reggie-2 were originally identified in the regenerating neurons of goldfish optic nerves [9] and later in endothelial cells, where they were termed flotillin-2 and flotillin-1 (flo-1) respectively [5] [6]. In addition to their postulated role in neuronal regeneration, flotillin-1/reggie-2 has been implicated in insulin signaling that triggers glucose transporter redistribution in adipocytes [10]. Flotillin-1 also associates with phagosomes in macrophages [11]. *Flotillin-1* and *flotillin-2* are highly conserved genes with orthologs in mouse, rat, human, fish and *Drosophila* [7,9,12–14]. We have observed *flotillin-1* overexpression in Sertoli cell cultures when cell interactions are chemically altered (manuscript in preparation).

The present paper analyzes the regulation of *flo-1* by cell–cell interactions in a cultured NIH-3T3 fibroblast experimental model. The pattern of mRNA and protein accumulation was followed after disruption of cell–cell interactions through to the re-establishment of intercellular contacts. The differential localization of flo-1 in the membrane and hydrophilic fractions of cell extracts – depending on cell interactions – suggests new roles for flo-1 in the cell.

The mouse promoter region of *flo-1* was also isolated and characterized in order to study the regulatory motifs possibly involved in the modulation of *flo-1* expression.

2. Materials and methods

2.1. Gene isolation and characterization

A cDNA clone corresponding to the *flo-1* gene was isolated in gene regulation experiments involving Sertoli cell cultures (data not shown).

From a mouse genomic library constructed in lambda phages, two overlapping phages were isolated and restriction-digested for mapping (Fig. 1). Sequence analysis of both phages and database comparisons showed a sequence corresponding to the first eight exons of *flo-1*, an upstream region corresponding to the *flo-1* promoter region, and the *gly96* gene.

Sequencing was carried out with an ABI Prism 3700 DNA analyzer (Applied Biosystems). Sequence comparisons were performed by nucleotide BLAST at the NCBI (http://www.ncbi.nlm.nih.gov/BLAST/).

*Corresponding author. Fax: (34)-91-5360432.
E-mail address: jdelmazo@cib.csic.es (J. del Mazo).

[1] The nucleotide sequence data reported are available in the GenBank database under accession numbers AY167925 and AY168443.

Abbreviations: flo-1, flotillin-1; PCR, polymerase chain reaction; SDS–PAGE, sodium dodecyl sulfate polyacrylamide gel electrophoresis; EST, expressed sequence tag; Sp1, Sp1 transcription factor; Lyf-1, zinc finger protein, subfamily 1a, 1 (Ikaros); MZF1, myeloid zinc finger protein 1; AML-1a, acute myeloid leukemia 1a; c-Ets-1, cellular progenitor of viral oncogene from E26 acute leukemia retrovirus (v-Ets); PHB, prohibitin-like domain

0014-5793/03/$22.00
doi:10.1016/S0014-5793(03)01239-0

2.2. Reporter gene constructs

Fusion gene constructs were made between *flo-1* promoter fragments and the *luciferase* reporter gene (Fig. 3). The promoter fragments fP1 (556 bp from nucleotide 4079 to 4634 in AY168443), fP2 (412 bp from nucleotide 4223 to 4634 in AY168443) and fP4 (173 bp from nucleotide 4462 to 4634 in AY168443) were obtained by polymerase chain reaction (PCR) using phage *λ31a1* from the genomic library (see Section 3) as a template. Specific primers were designed from the putative promoter region. The reverse primer was the same in all primer combinations; it carried a *Bgl*II target sequence at the 5′ end (small letters in fP-R sequence). The oligonucleotide sequences were: fP1-F, 5′-CTGTGAACACGAATAAACTT-3′ (forward); fP2-F, 5′-CTTGGAGTTACAGACCTATA-3′ (forward); fP4-F, 5′-GGCTGCCGAGAACTGTA-3′ (forward); fP-R, 5′-gaagatcttcAACGGGGTGGGGACTGC-3′ (reverse).

The PCR profile was: 10 min at 95°C, 35 cycles of 15 s at 95°C, 30 s at 60°C and 1 min at 72°C, and an additional elongation step for 10 min at 72°C. All PCR products were cloned in pGEM-T Easy vector (Promega), according to the manufacturer's instructions. Inserts from each plasmid construct were released by *Eco*RI and *Bgl*II digestion. Purified inserts were then cloned in *luciferase* expression vector pGL3-basic (Promega). All resultant constructs were verified by sequencing.

2.3. Culture and transient transfection of NIH-3T3 cells

Mouse embryonic fibroblasts NIH-3T3 were cultured in a 5% CO_2/95% air atmosphere at 37°C in Dulbecco's modified Eagle's medium (Gibco BRL) supplemented with 10% heat-inactivated fetal bovine serum, 2 mM L-glutamine, 100 U/ml penicillin, and 100 μg/ml streptomycin.

Confluent NIH-3T3 cells cultured in 100×20 mm Style Standard dishes (BD Falcon) were detached by trypsin treatment. Dissociated cells were then distributed into new dishes (8×10^5 cells/dish) and allowed to grow for 96 h to regain confluence. Total RNA samples were obtained from trypsinized cells at 24 h, 48 h, 72 h and 96 h.

Subconfluent NIH-3T3 cells growing in 12-well cell culture plates (BD Falcon) were transiently cotransfected with 1 μg of recombinant pGL3-basic constructs plus 0.2 μg of *RSV-β-Gal* plasmid as an internal control for transfection efficiency. As a vehicle for transfection, the FuGENE 6 transfection reagent (Roche Applied Science) was used following the manufacturer's instructions. After 24 h, cell lysates were prepared from the transfected cells using Passive Lysis Buffer (Promega). As a negative control of promoter activity we also transfected empty pGL3-basic. Each experiment was replicated at least three times. Luciferase activity was measured in cell lysates with the Luciferase Assay System (Promega) using a luminometer (TD-20/20, Promega) according to the manufacturer's instructions. β-Galactosidase activity was assayed according to standard procedures [15] with *o*-nitrophenyl-β-D-galactopyranoside; A_{420} was measured in an automated ELISA reader (Labsystems Multiskan Bichromatic, Helsinki, Finland).

2.4. Northern blots

Total RNA from NIH-3T3 cell cultures at different stages of growth (see Section 3) were extracted by RNAwiz (RNA isolation reagent [Ambion]) following the manufacturer's instructions. The mRNA samples (15 μg) were electrophoretically separated under denaturing conditions (1% agarose/8% formaldehyde) and transferred to nylon. Prehybridization and hybridization with [α-^{32}P]dCTP-labeled *flotillin-1* and *S16 ribosomal protein* cDNAs were performed in Church solution [16] for 1 h at 65°C and overnight at 68°C respectively. Membranes were washed and X-ray film exposed for 3 days at −80°C. [α-^{32}P]dCTP-labeled *S16 ribosomal protein* cDNA was used as a probe for the loading control [17].

2.5. Western blots

To analyze the flotillin-1 protein in NIH-3T3 cells we prepared protein extracts from the hydrophobic (membrane) and hydrophilic fractions using the Mem-PER Eukaryotic Membrane Protein Extraction Reagent kit (Pierce). This kit is based on the separation of plasma membrane proteins by the technique of aqueous two-phase partition [18–20]. Protein fractions obtained from 7×10^4 cells from trypsinized cultures at different growth stages (see Section 3) were separated by sodium dodecyl sulfate–polyacrylamide gel electrophoresis (SDS–PAGE) on 12% polyacrylamide gels [21] and electrophoretically transferred to polyvinylidene difluoride membranes according to Towbin [22]. A replica of protein separation (10% polyacrylamide gel) was visualized by Coomassie blue staining in order to check the loading (Fig. 5A). Filters were probed with mouse monoclonal antibody against flotillin-1 (BD Transduction Laboratories). As a control of the hydrophobic/hydrophilic protein separation, the filters were stripped and reprobed with rabbit polyclonal antibody against caveolin (BD Transduction Laboratories) as an integral membrane protein. We used peroxidase-conjugated anti-mouse IgG or anti-rabbit IgG (Amersham Biosciences) as secondary antibodies. The blots were developed using the ECL Western blotting analysis system (Amersham Biosciences) and exposed to X-ray film.

3. Results

3.1. Characterization of the mouse flotillin-1 gene and promoter region

From a cDNA clone corresponding to a differentially expressed gene in Sertoli cells (unpublished results), we screened a mouse testis cDNA library to isolate the full-length cDNA corresponding to the *flotillin-1* gene (GenBank accession number AY167925). The 1701 bp cDNA was used to screen a mouse genomic library using a *Pst*I restriction fragment (Fig. 1A). Two overlapping phages, *λ31a1* and *λ21a1*, were isolated and restriction-digested for mapping analysis (Fig. 1B).

A large fragment (8.2 kb) from *λ31a1* was sequenced (Fig. 1B) and submitted to GenBank (accession number AY168443). The genomic sequence was analyzed by comparison with the *flo-1* cDNA sequence and eight exons corresponding to the 5′ region of the gene were identified. Comparison with databases showed the presence of the gene *gly96* in the same strand upstream of *flo-1*. *gly96* is an immediate-early gene inducible by serum growth factors in mouse fibroblasts [23]. The chromosomal organization of both genes is conserved in the human genome where a *Ier3* (*immediate-early response 3*) ortholog flanks *Flotillin-1* in the 5′ position [24].

BLAST homology searches for expressed sequence tag (EST) sequences of this region revealed four ESTs corresponding to the 5′ region of *flo-1* that do not carry exon 4 in normal nervous tissue (olfactory epithelium, accession number BU148641, and neonate cortex, accession number BB873447). The same exon 4 deletion was observed for ESTs corresponding to mammary tumor (accession numbers BI156168 and BI157452).

To identify the promoter region of the mouse *flo-1* gene, the 456 bp nucleotide sequence of the 5′ flanking region (nucleotides 4096–4551 in AY168443) was analyzed to search for possible transcription factor binding sites with a threshold score of 90 (Y. Akiyama: 'TFSEARCH: Searching Transcription Factor Binding Sites', http://www.rwcp.or.jp/papia/ [25]). After computer analysis with mouse 5′ EST databases, our cDNA was found to be the longest at the 5′ end; the first nucleotide for transcription was taken to be that at position 4552 (AY168443). This 456 bp region lacks a consensus TATA box, as occurs in the human ortholog, but several putative transcription factor binding sites were found (Fig. 2).

There is a putative CpG island (69.18% CG content) spanning from nucleotide 4461 to 4739 in AY168443, 72% identical to the human *Flotillin-1* CpG island [24]. The mouse CpG island (279 bp) is shorter than the human version (545 bp) but its location in the gene structure (covering exon 1) is the same (Fig. 3).

To characterize the promoter, we prepared a series of recombinant plasmids containing different portions of the

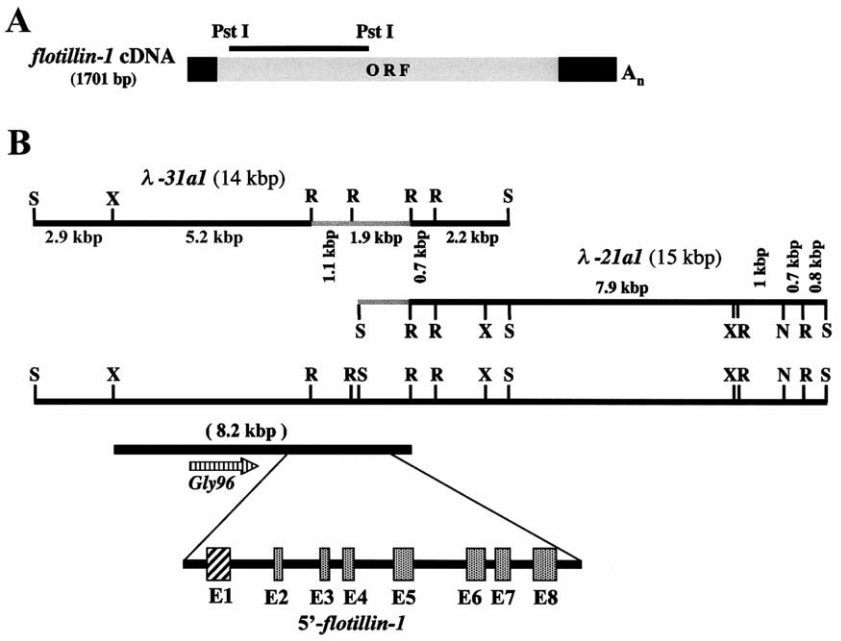

Fig. 1. Isolation of the *flotillin-1* promoter region. A: Diagram showing the location of the *Pst*I restriction fragment in the full-length *flotillin-1* cDNA used as a probe in genomic screening. B: Restriction maps of the overlapping clones obtained from the mouse genomic library: *λ31a1* and *λ21a1*. The *Pst*I probe hybridized with the restriction fragments marked in gray in both phage maps. Below is shown the 8.2 kb sequenced region with the location of the *gly96* gene and the first eight exons of the *flotillin-1* gene. S, *Sau*3AI; R, *Eco*RI; X, *Xba*I; N, *Not*I.

5′ flanking *flo-1* sequence inserted upstream of the *luciferase* coding region. These were used in transient cotransfection experiments with NIH-3T3 cells using a *β-galactosidase*-encoding plasmid as the transfection control. Fig. 3 shows how all constructs were able to trigger the transcription of *luciferase*. The shorter segment (fP-4) covering the 5′ end of the CpG island and including the putative Sp1 transcription factor (Sp1) and zinc finger protein, subfamily 1a, 1 (Ikaros) (Lyf-1) binding sites led to only basal transcription. The fP-2 segment, with a second Sp1 binding site, a CAAT box and putative specific binding sites for myeloid zinc finger protein 1 (MZF1), acute myeloid leukemia 1a (AML-1a) and cellular progenitor of viral oncogene from E26 acute leukemia retrovirus (c-Ets-1) produced about twice as much luciferase activity as fP-4. The larger segment, fP-1, which additionally contained a putative MZF1 binding site, promoted about twice as much luciferase activity as the fP-2 construct and almost six times as much as fP-4. No activity was detected in the lysate of cells transfected with the empty pGL3-basic plasmid.

```
-473  ctgtgaacacgaataaacttgatttgcctgtcattattatctgcagttctcgaagtgtat
-413  cattcaggcgggggggaggggggagtgacgggaggatgtgactaggtgcccagtcctcac
                    MZF1
-353  cctttcttgggtcctgaactctttcttggagttacagacctatatccggtcaccggatgc
                                                        c-Ets-1
-293  agtcatacattgctgggtgtgcggttttcccagttagagagtggtgtggcaacctgctta
                         AML-1a
-233  ctcatggcaggcggcgggtattcaggaaccagagtggaagggcgtggcctcggttggggg
-173  cggagcttccacgccaatgcttcgagcgggggggggggggggggttggttgttggtgggg
               CAAT-Box                Sp1                   MZF1
-113  ggagaatgtctggcatcccccctgggctgccgagaactgtagtgctgcggacccgagcgga
                                                          +1
 -53  gcctgccgggaaaggggcggaccgaggggttgggaggggcggggtcgcgtctGTTGCTG
                          Lyf-1      Sp1
   +8  CAACAGGGTGCGGCCGGGTGGGGGGCGCAAGTGCAGCTTCCACTAAGCCGGGTGTCCGAG
  +68  CAGTCCCCACCCCGTTCTGGGGTTCTGCGGGCCTCCGCGCTTCTCAAGACCCCGGTGGGG
                                  ▼
 +128  TTGCTTACGGGGACGTTCCGGAAGGTGAGTGGGGATGGGAGGCGGAGCCTTGGGCTACTG
 +188  AAGAGCCTGGAGGCTGCGGAACTGCTGCAGACCCCTGGGCGCGGGAGAGCTTTGTGTGGT
 +248  AGAGGGGCTAGGGGGCGCGGTGAGAGGAAGACTGTGAGAATCAACTGGCACAGAGGAAGA
 +308  AGTCCCGGGGGGGGGGGTGTCTTAGGACTGTCACAGGGGCGCTCAAGGGACTGGGCGGTG
 +368  GCAGAGGCAGTTGGTGCTCCTGATAGGAGGGTAAGGAGGTGCCACAGGGCCCCTTCCCCT
 +428  TTGCAAAGGCTTCCTCTCTATTCCTCTCCAG
```

Fig. 2. Nucleotide sequence of the *flotillin-1* promoter. The promoter region is written in lower case letters and extends from the *gly96* polyadenylation signal (marked in italics and bold) to the *flotillin-1* transcription start site (marked by ↓). Putative binding sites for transcription factors are underlined and indicated. The putative CpG island is shown in italics. The boundary between exon 1 and intron 1 is marked with a solid triangle.

3.2. *The expression of* flotillin-1 *mRNA and protein is related to cell–cell interaction*

Abundant *flo-1* RNA expression was detected in NIH-3T3 fibroblasts compared to that reported for other cells and tissues [5]. We therefore took this cell type as a model system to evaluate the regulation of *flo-1* expression mediated by cell–cell interactions.

We analyzed the level of gene expression by mRNA accumulation in cells cultured at confluence when all cell interactions are fully established. These interactions were disrupted by trypsinization and new cultures were established. After 24 h of subculture, about 50% of the dish surface was occupied by growing cells. At this stage, the level of *flo-1* expression was reduced to one third of its value at confluence (Fig. 4, lane 2). At 48 h of culture, about 75% plate occupancy was observed and the level of *flo-1* was double that at 24 h (Fig. 4, lane 3). The maximum was reached at 72 h and 96 h when 100% confluence was achieved in the culture dishes (Fig. 4, lanes 4 and 5). The level of mRNA at 96 h was the same as the level of expression detected in trypsinized confluent cells (Fig. 4, lane 1).

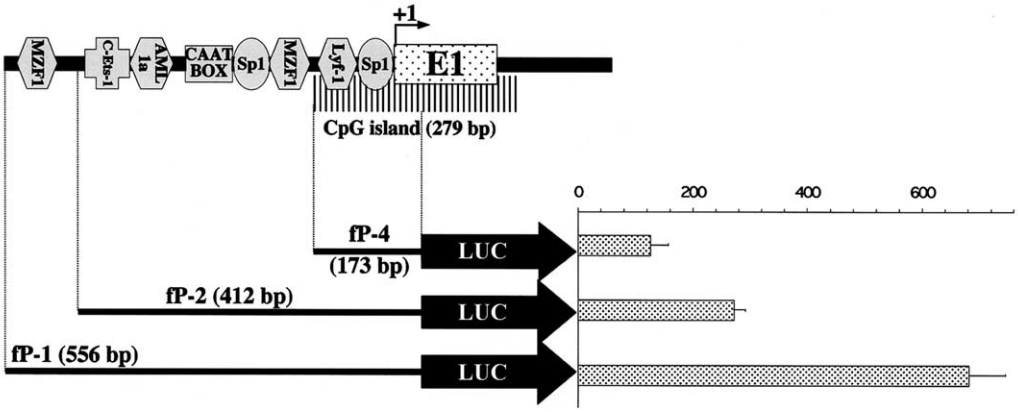

Fig. 3. Functional analysis of the *flotillin-1* promoter region. Diagram representing the *flotillin-1* promoter region with the location of putative binding sites for transcription factors. The promoter activities of the constructs with the *luciferase* reporter transiently transfected into NIH-3T3 cells are also shown. Left: The locations and sizes of the tested promoter fragments. Right: Luciferase activity as X-fold value compared to cells transfected with the promoterless pGL3-basic vector normalized with β-galactosidase activity (transfection efficiency control). Data are the mean and S.D. of triplicates.

To check whether the *flo-1* mRNA regulation detected in NIH-3T3 cells correlated with an increase in protein expression, Western blot experiments were performed to detect flotillin-1 in both the hydrophilic and hydrophobic protein extracts from the stages described above. Protein fractions were obtained from a defined number of cells (7×10^4) in each experimental stage. Total protein balance between samples was visualized by Coomassie blue staining (Fig. 5A). In both the hydrophobic and the hydrophilic fractions, a progressive increase of flo-1 protein was detected associated with

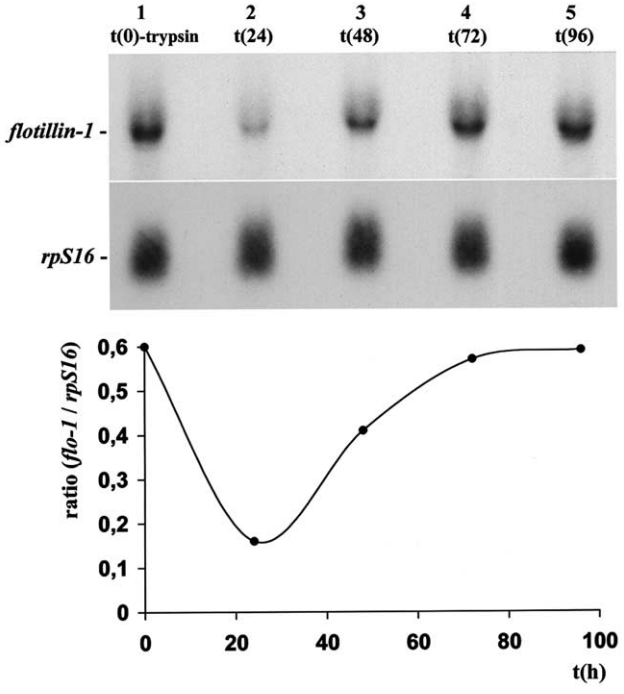

Fig. 4. Expression of the *flotillin-1* gene in NIH-3T3 cells at different levels of cell–cell interaction. Northern blot analysis was performed. Total RNA (15 μg) from cells growing at different levels of plate occupancy: (lane 1) RNA from cells at confluence, immediately processed after trypsinization; (lane 2) after 24 h of subculture the cells occupied about 50% of the plate surface; (lane 3) after 48 h of culture the cells occupied about 75% of the plate surface; lanes 4 and 5: cells were at confluence after 72 h and 96 h of culture respectively. Hybridization with *ribosomal protein S16* probe (*rpS16*) was performed as a loading control. A graphic representation is provided to indicate the dynamics of *flotillin-1* expression, from the disruption of NIH-3T3 cell interactions to their re-establishment. The *y*-axis shows the ratio between *flotillin-1* values from densitometric analyses and the corresponding value of *rpS16*.

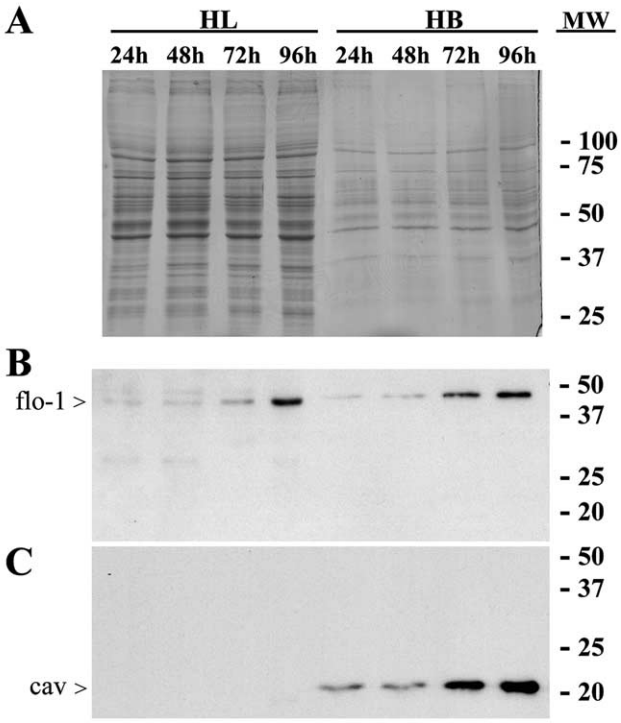

Fig. 5. A: Coomassie blue staining of SDS–PAGE of hydrophilic (HL) and hydrophobic (HB) fractions obtained from the same number of NIH-3T3 cells (see Section 2) growing in the same experimental conditions used for Northern blots (lanes 1 and 5, 24 h; lanes 2 and 6, 48 h; lanes 3 and 7, 72 h; lanes 4 and 8, 96 h). B: Western blot that shows the accumulation of flotillin-1 (flo-1) in the hydrophilic and membrane fractions at sequential stages of NIH-3T3 cell–cell interactions. C: Detection of the integral membrane protein caveolin (cav) as a control of efficiency in the hydrophobic/hydrophilic separation. It is interesting to note that caveolin increases in the membrane fraction in correlation with flotillin-1. Molecular weight markers are indicated.

the increase of cell–cell interactions (Fig. 5B). Intriguingly, in the early stages (24 and 48 h, i.e. before cell confluence) there was less protein in the hydrophilic than in the hydrophobic fraction, but this was reversed at 96 h (at confluence) (Fig. 5B). Additionally, as is shown in Fig. 5C, the integral membrane protein caveolin was only present at the hydrophobic fraction; this fact proves the efficiency of the protein extraction method. Therefore, these experiments demonstrate that there is a remarkable accumulation of flo-1 outside the membrane in addition to its membrane localization. Moreover, we detected a progressive increase of caveolin towards cells at confluence (Fig. 5C).

These data demonstrate that the level of accumulation of *flotillin-1* transcripts and protein is correlated.

4. Discussion

Our observation of *flo-1* deregulation in Sertoli cell culture might be associated with disorganization of cell–cell interactions (manuscript in preparation). Here, we show that establishing cell interactions in an NIH-3T3 culture model mediates the regulation of *flo-1* expression. The correlation between cell–cell interactions and *flo-1* expression level was hypothesized following experiments on axon regeneration in the retinal ganglion cells of goldfish [9]. In these experiments, Schulte et al. showed that the *flo-1* goldfish ortholog, *reggie-2*, is upregulated in retinal ganglion cells during normal axon growth and regeneration following optic nerve injury. The growing axons must establish new interactions with the environment on the way to their target cells. The same has been shown in rat retinal ganglion cells [7]. In addition, reggie-2 has been localized, at both light and electron microscopic levels, at cellular contact sites in cultured, differentiated rat adrenal pheochromocytoma PC12 neural cells (7 days in the presence of nerve growth factor) [8].

In our experiments, the modifications carried out in the culture system were based on the disruption and restoration of cell contacts. When cell–cell interactions were disrupted, the level of *flo-1* mRNA and protein decreased significantly. Therefore, the increase in the level of both mRNA and protein was concomitant with the restoration of these interactions. This suggests a direct participation of flo-1 in the establishment of cell–cell interactions – or that it is a consequence of it. According to the participation of flo-1 in the establishment of cell adhesion structures, c-Cbl-associated protein/ponsin and vinexin-α, two mammalian members of the recently described adapter protein family vinexin [26], must have the ability to bind flo-1 throughout their sorbin homology domain in their N-terminal regions. These proteins also contain three Src homology 3 domains in their C-terminal region, which allow binding to specific signaling and cytoskeletal molecules. In addition, it has been described that these adapter proteins have a role in cell adhesion and cytoskeletal organization through their binding to vinculin, an actin binding cytoskeletal protein localized in the cell–extracellular matrix and at cell–cell adhesion sites [26]. Further experiments must be performed to verify this interaction pathway, which would support the relationship between lipid rafts at the plasma membrane and the setting up of cellular adhesion structures via flo-1.

Flo-1 has largely been described as a plasma membrane-associated protein and, consequently, it should mainly be found in the hydrophobic cell fraction. However, in our protein analysis, we observed that the flo-1 content of the hydrophilic fraction was also significantly increased during culture growth from 24 h to 96 h (Fig. 5B). This high accumulation of flo-1 outside the membrane has not been reported before. The hydrophilic fraction of cells that reached total confluence, at 72 h or 96 h, contained higher flo-1 levels than cells at 24 h or 48 h when cell–cell interactions were not fully established. Moreover, flo-1 levels at 96 h in the hydrophilic fraction were equivalent or higher than in the hydrophobic fraction (Fig. 5B). These results indicate that flo-1 is both a strongly membrane-associated protein (hydrophobic protein fraction) and a peripheral or putatively cytoplasmic protein (hydrophilic protein fraction) in NIH-3T3 cells. Morrow and colleagues [27] support the hypothesis that flo-1 associates with the cytoplasmic face of the plasma membrane via a novel plasma membrane targeting mechanism involving the prohibitin-like domain (PHB) and palmitoylation sites in the N-terminal region of the flo-1 protein. The hydrophobic PHB domain acts like a lipid raft recognition motif, which targets the flo-1 protein to the plasma membrane via a Golgi-independent trafficking pathway. In addition, the association of flo-1 with the plasma membrane is dependent on protein palmitoylation. Further, the significance of protein palmitoylation in lipid raft targeting has been recognized owing to the existence of regulated depalmitoylation in response to certain stimuli that might imply protein translocation from the membrane to the cytoplasm [28]. Our results showing enrichment of flo-1 in the hydrophilic fraction in a manner related to cell–cell interactions might be explained in two ways: (a) profuse amounts of flo-1 in the hydrophilic fraction could be due to the saturation of protein at the membrane rafts when cell contacts are fully established; (b) regulated translocation from the membrane to the cytoplasm could take place in response to stimuli derived from the establishment of cell–cell interactions. Based on these results, the functional significance of flo-1 protein outside the membrane should be explored in further studies. Our results with caveolin confirm a previous report about the increase of this protein also associated with cell–cell interactions [29].

To analyze expression of the regulatory regions acting at *cis* in the *flo-1* gene, we isolated and characterized the genomic region corresponding to its promoter, and analyzed the 5′ flanking sequence of the *flo-1* transcription start site. This promoter region contained a 279 bp putative CpG island highly conserved in sequence and location, although it was somewhat shorter than that described for the human *flo-1* CpG island [24]. No TATA box consensus sequence was found in this promoter region, as in the human gene. In contrast, a CAAT box was found at an expected site, related to the transcription start site (Figs. 2 and 3). We also found two consensus Sp1 binding sites near the transcription start site, one located within the CpG island. Intriguingly, we found several binding sites for transcription factors that are mostly involved in the regulation of hematopoietic cell differentiation: AML-1a [30] and MZF1 [31] in myeloid cell differentiation, and c-Ets-1 [32] and Lyf-1 [33] in lymphoid cell differentiation. The presence of binding sites for these transcription factors is in agreement with the presence of flo-1 in monocytes, in the lipid rafts of the macrophage-like cell line J774 [11,34], in those of Jurkat T cells [8], and in erythrocyte plasma membranes [35]. In erythrocytes, flo-1 was detected as one

of the major proteins associated with lipid rafts, together with stomatin and flotillin-2. No evidence was found for elements binding specific transcription factors that might explain the pattern of *flo-1* expression after the disruption of NIH-3T3 cell–cell interactions. Nevertheless, in the luciferase functional assays, the presence of a second element for MZF1 binding in the fP-1 construct, with respect to fP-2, was sufficient to increase luciferase activity to more than twice that of the other domains analyzed in the NIH-3T3 cells transfected (Fig. 3). Therefore, this short 5′ promoter fragment might play an important role in enhancing *flo-1* expression.

Evidence for alternative splicing of the *flo-1* transcript was detected in specific tissues after databank analysis. This has not been described in humans [24]. We found several EST sequences (see Section 3 for accession numbers) in databases corresponding to the *flo-1* gene with exon 4 deleted (in mammary tumor, olfactory epithelium, and neonate cortex mouse expression libraries). The mRNA lacking the exon 4 would theoretically encode a truncated flo-1 at the C-terminal end. However, an alternative open reading frame would encode the whole flo-1 except for the first 79 amino acids of the N-terminal end. This N-terminal region would correspond to part of the described PHB domain [27]. The significance of this putative alternative splicing should be analyzed in further experiments.

In conclusion, (i) in NIH-3T3 cells with established cell–cell interactions the expression of *flotillin-1* is modulated depending on the level of these interactions. This confers upon *flotillin-1* a potential role in cell processes where cellular interactions may be required for normal or pathological conditions; (ii) the conspicuous presence of flotillin-1 outside its classically defined location in the membrane may provide new ways to study its role in the cell; (iii) the promoter region of *flotillin-1*, with its specific regulatory domains, has been defined. This may help in further studies on the regulation and function of this protein.

Acknowledgements: The authors thank J.F. Escolar for technical assistance and Dr. Maria Paz for her suggestions with the Western blot analysis. This work was supported by grants from the CICYT (BMC2000-1127), EU (QLK4-CT-2002-02403) and PROFIT (FIT-010000-2002-43) to J.M.

References

[1] Brown, D.A. and Rose, J.K. (1992) Cell 68, 533–544.
[2] Razani, B., Woodman, S.E. and Lisanti, M.P. (2002) Pharmacol. Rev. 54, 431–467.
[3] Kurzchalia, T.V. and Parton, R.G. (1999) Curr. Opin. Cell Biol. 11, 424–431.
[4] Harris, T.J. and Siu, C.H. (2002) BioEssays 24, 996–1003.
[5] Bickel, P.E., Scherer, P.E., Schnitzer, J.E., Oh, P., Lisanti, M.P. and Lodish, H.F. (1997) J. Biol. Chem. 272, 13793–13802.
[6] Volonte, D., Galbiati, F., Li, S., Nishiyama, K., Okamoto, T. and Lisanti, M.P. (1999) J. Biol. Chem. 274, 12702–12709.
[7] Lang, D.M. et al. (1998) J. Neurobiol. 37, 502–523.
[8] Stuermer, C.A., Lang, D.M., Kirsch, F., Wiechers, M., Deininger, S.O. and Plattner, H. (2001) Mol. Biol. Cell 12, 3031–3045.
[9] Schulte, T., Paschke, K.A., Laessing, U., Lottspeich, F. and Stuermer, C.A. (1997) Development 124, 577–587.
[10] Baumann, C.A. et al. (2000) Nature 407, 202–207.
[11] Dermine, J.F., Duclos, S., Garin, J., St-Louis, F., Rea, S., Parton, R.G. and Desjardins, M. (2001) J. Biol. Chem. 276, 18507–18512.
[12] Galbiati, F. et al. (1998) Gene 210, 229–237.
[13] Hazarika, P., Dham, N., Patel, P., Cho, M., Weidner, D., Goldsmith, L. and Duvic, M. (1999) J. Cell Biochem. 75, 147–159.
[14] Malaga-Trillo, E., Laessing, U., Lang, D.M., Meyer, A. and Stuermer, C.A. (2002) J. Mol. Evol. 54, 235–245.
[15] Ausubel, F.M. (1998), Current protocols in molecular biology, John Wiley and Sons, New York.
[16] Church, G.M. and Gilbert, W. (1984) Proc. Natl. Acad. Sci. USA 81, 1991–1995.
[17] Wagner, M. and Perry, R.P. (1985) Mol. Cell. Biol. 5, 3560–3576.
[18] Lenstra, J.A. and Bloemendal, H. (1983) Eur. J. Biochem. 135, 413–423.
[19] Morre, D.J. and Morre, D.M. (1989) BioTechniques 7, 946–948, 950–954, 956–958.
[20] Ohlendieck, K. (1996) Methods Mol. Biol. 59, 293–304.
[21] Laemmli, U.K. (1970) Nature 227, 680–685.
[22] Towbin, H., Staehelin, T. and Gordon, J. (1979) Proc. Natl. Acad. Sci. USA 76, 4350–4354.
[23] Charles, C.H., Yoon, J.K., Simske, J.S. and Lau, L.F. (1993) Oncogene 8, 797–801.
[24] Edgar, A.J. and Polak, J.M. (2001) Int. J. Biochem. Cell Biol. 33, 53–64.
[25] Heinemeyer, T. et al. (1998) Nucleic Acids Res. 26, 362–367.
[26] Kioka, N., Ueda, K. and Amachi, T. (2002) Cell. Struct. Funct. 27, 1–7.
[27] Morrow, I.C., Rea, S., Martin, S., Prior, I.A., Prohaska, R., Hancock, J.F., James, D.E. and Parton, R.G. (2002) J. Biol. Chem. 277, 48834–48841.
[28] Resh, M.D. (1999) Biochim. Biophys. Acta 1451, 1–16.
[29] Galbiati, F., Volonte, D., Engelman, J.A., Watanabe, G., Burk, R., Pestell, R.G. and Lisanti, M.P. (1998) EMBO J. 17, 6633–6648.
[30] Niitsu, N., Yamamoto-Yamaguchi, Y., Miyoshi, H., Shimizu, K., Ohki, M., Umeda, M. and Honma, Y. (1997) Cell Growth Differ. 8, 319–326.
[31] Hromas, R., Collins, S.J., Hickstein, D., Raskind, W., Deaven, L.L., O'Hara, P., Hagen, F.S. and Kaushansky, K. (1991) J. Biol. Chem. 266, 14183–14187.
[32] Chen, J.H. (1990) Oncogene Res. 5, 277–285.
[33] Lo, K., Landau, N.R. and Smale, S.T. (1991) Mol. Cell. Biol. 11, 5229–5243.
[34] Li, N., Mak, A., Richards, D.P., Naber, C., Keller, B.O., Li, L. and Shaw, A.R. (2003) Proteomics 3, 536–548.
[35] Salzer, U. and Prohaska, R. (2001) Blood 97, 1141–1143.